NASA TECHNICAL REPORT

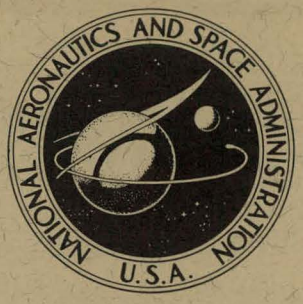

NASA TR R-178

NASA TR R-178

THEORETICAL DETERMINATION OF THE BOUNDARY AND DISTORTION OF THE GEOMAGNETIC FIELD IN A STEADY SOLAR WIND

by Benjamin R. Briggs and John R. Spreiter
Ames Research Center
Moffett Field, Calif.

NATIONAL AERONAUTICS AND SPACE ADMINISTRATION - WASHINGTON, D. C. - SEPTEMBER 1963

DISCLAIMER

TECHNICAL REPORT R-178

THEORETICAL DETERMINATION OF THE BOUNDARY AND DISTORTION OF THE GEOMAGNETIC FIELD IN A STEADY SOLAR WIND

By Benjamin R. Briggs and John R. Spreiter

Ames Research Center
Moffett Field, Calif.

NATIONAL AERONAUTICS AND SPACE ADMINISTRATION

NATIONAL AERONAUTICS AND SPACE ADMINISTRATION

TECHNICAL REPORT R-178

THEORETICAL DETERMINATION OF THE BOUNDARY AND DISTORTION OF THE GEOMAGNETIC FIELD IN A STEADY SOLAR WIND

By Benjamin R. Briggs and John R. Spreiter

ABSTRACT

An approximate formulation of the steady-state Chapman-Ferraro problem, given recently by Davis and Beard, is used to calculate the coordinates of the complete boundary of the geomagnetic field. Field lines are then computed in the magnetic meridian plane containing the free-stream direction of the solar wind, taking into account the distorting effects of currents flowing in the boundary. Numerical results are given for the case where the geomagnetic dipole axis is perpendicular to the direction of the solar wind.

NATIONAL AERONAUTICS AND SPACE ADMINISTRATION

TECHNICAL REPORT R-178

THEORETICAL DETERMINATION OF THE BOUNDARY AND DISTORTION OF THE GEOMAGNETIC FIELD IN A STEADY SOLAR WIND

By Benjamin R. Briggs and John R. Spreiter

SUMMARY

An approximate formulation of the steady-state Chapman-Ferraro problem, given recently by Davis and Beard, is used to calculate the coordinates of the complete boundary of the geomagnetic field. Field lines are then computed in the magnetic meridian plane containing the free-stream direction of the solar wind, taking into account the distorting effects of currents flowing in the boundary. Numerical results are given for the case where the geomagnetic dipole axis is perpendicular to the direction of the solar wind.

INTRODUCTION

This paper is concerned with the theoretical determination of the steady-state shape and location of the interface, or boundary, between the magnetosphere and the solar wind, and of field lines in the confined geomagnetic field. Recent accounts of the basic physics, and of the formulation of unsteady as well as steady-state mathematical models relating to this problem, will be found in references 1 through 5.

The present work is an extension of that reported in references 6 through 13 wherein the three-dimensional Chapman-Ferraro problem is simplified by the introduction of an approximate boundary condition. The coordinates of the entire boundary of the magnetosphere are calculated for the case in which the dipole axis is perpendicular to the free-stream direction. A number of field lines are then computed in the magnetic meridian plane containing the free-stream direction, taking into account the effect of electric currents in the boundary.

COMPUTATION OF THE COORDINATES OF THE BOUNDARY

FORMULATION OF THE PROBLEM

The determination of the shape of the boundary of the geomagnetic field, and the total magnetic field $\underset{\sim}{B}$ inside it, involves the solution of the magnetic field equations $\operatorname{div} \underset{\sim}{B} = 0$ and $\operatorname{curl} \underset{\sim}{B} = 0$. The earth's magnetic field is represented by a three-dimensional dipole singularity at the origin (the center of the

earth). The normal component of $\underset{\sim}{B}$ vanishes at the boundary, and Dungey (ref. 3) has shown that the total (tangential) field at the boundary, B_s, may be expressed mathematically by the relation

$$\frac{B_s^2}{8\pi} = 2mnv^2 \cos^2 \psi \tag{1}$$

The quantities m, n, and v are mass, number density, and velocity of the positive ions in the solar stream, and ψ is the angle between the free-stream velocity vector and an outward normal to the surface. The condition $\cos \psi \leq 0$ must hold on the boundary.

It is a property of the boundary-value problem described above that the field $\underset{\sim}{B}$ can vanish only at isolated points on the boundary. These points are designated neutral points. It follows from equation (1) that $\cos \psi$ vanishes, and the boundary is therefore parallel to the stream, at these points.

Beard (ref. 6) dropped the condition that the normal component of $\underset{\sim}{B}$ vanishes at the boundary and replaced it with the approximate condition that $B_s = 2B_t$, where B_t is the tangential component of the geomagnetic dipole field $\underset{\sim}{B}_p$ at the boundary. The closely related approximation, suggested by Ferraro (ref. 9),

$$B_s = 2fB_t \tag{2}$$

where f is a constant, was used by Spreiter and Briggs (refs. 10, 11, and 12) and is employed in the present work.

The differential equation that defines the shape of the boundary of the magnetosphere according to this approximation is obtained by substitution of equation (2) into equation (1). It is, following Davis and Beard (ref. 13),

$$\left[\frac{1+3\cos^2\theta}{\rho^6}\left(\frac{1}{\rho \sin\theta}\frac{\partial\rho}{\partial\varphi}\right)^2 + \frac{1}{\rho^6}\left(\sin\theta + \frac{2\cos\theta}{\rho}\frac{\partial\rho}{\partial\theta}\right)^2\right]$$

$$= \left(\sin\varphi \sin\theta - \frac{\sin\varphi\cos\theta}{\rho}\frac{\partial\rho}{\partial\theta} - \frac{\cos\varphi}{\rho\sin\theta}\frac{\partial\rho}{\partial\varphi}\right)^2 \tag{3}$$

where $\rho = r/r_o$ and

$$r_o = \left(\frac{4f^2M_p^2}{16\pi mnv^2}\right)^{1/6} = a\left(\frac{4f^2B_{p_o}^2}{16\pi mnv^2}\right)^{1/6} \tag{4}$$

The variables r, θ, and φ are spherical coordinates that are fixed with respect to the geomagnetic dipole axis (see fig. 1). The quantity M_p, the magnetic moment of the dipole, is equal to $a^3 B_{p_o}$, where a represents the radius of the earth, and B_{p_o} is the magnitude of $\underset{\sim}{B}_p$ at the magnetic equator on the surface of the earth. The quantities in equation (4) are in cgs units, and numerical values for a, B_{p_o}, and m are 6.37×10^8 cm, 0.312 gauss, and 1.67×10^{-24} gram (for protons), respectively.

The quantity r_o is the geocentric distance along the sun-earth line to the boundary of the geomagnetic field. Representative quiet time values for v and n are 500 km/sec and 2.5 protons/cm^3, according to preliminary analysis of data from Mariner II (Neugebauer and Snyder, ref. 14). These lead to a value for r_o of 9.6 earth radii for $f = 1$. Axford (ref. 15) (see also Kellogg, ref. 16) has suggested that if the weak interplanetary magnetic field is taken into account, a collision-free shock wave may exist in the solar stream on the sunward side of the magnetosphere. A consequence of the presence of such a shock wave is that the dimensions of the boundary are greater by a factor of $2^{1/6}$ than those indicated for the present model. Thus the value for r_o would be about 10.8 earth radii in the example given above.

If attention is confined to the plane $\varphi = \pm\pi/2 (x = 0)$ where the derivative $\partial\rho/\partial\varphi$ is zero by consideration of symmetry, equation (3) reduces to an ordinary differential equation that can be solved analytically. The trace of the boundary in this plane is illustrated in figure 2(a). The front portion is circular, $\rho = 1$, and the upper portion is defined by the relation

$$\rho \cos \theta = (3/2^{2/3})\rho^3/(1 + \rho^3)$$

The point labeled N is the point of intersection of the two segments of this trace. It corresponds to a neutral point of the solution of the exact Chapman-Ferraro problem, since the magnetic field indicated by equation (2) is directed in opposite directions on either side of these points. All field lines in the boundary converge to the neutral points, turn sharply, and extend to the earth. The magnitude of the magnetic field should be zero at the neutral points in the boundary, although this condition is not fully attained in the approximate solution given here.

The trace in the plane $\theta = \pi/2 (z = 0)$, the magnetic equatorial plane, is obtained similarly by solving numerically the ordinary differential equation to which equation (3) reduces in this case. Tabulations of this result are given by Beard (ref. 6) and by Spreiter and Briggs (ref. 10). It is illustrated in figure 2(b).

Notice that the derivatives $\partial\rho/\partial\theta$ and $\partial\rho/\partial\varphi$ appear to the second power in equation (3). Thus, it may be rewritten conveniently in either the form

$$A_1 \left(\frac{1}{\rho}\frac{\partial\rho}{\partial\theta}\right)^2 + A_2 \left(\frac{1}{\rho}\frac{\partial\rho}{\partial\theta}\right) + A_3 = 0 \qquad (5)$$

or

$$B_1 \left(\frac{1}{\rho \sin\theta}\frac{\partial\rho}{\partial\varphi}\right)^2 + B_2 \left(\frac{1}{\rho \sin\theta}\frac{\partial\rho}{\partial\varphi}\right) + B_3 = 0 \tag{6}$$

Here

$$\left.\begin{aligned} A_1 &= \cos^2\theta \left(\sin^2\varphi - \frac{4}{\rho^6}\right) \\ A_2 &= -2\cos\theta \left[\sin\theta \left(\sin^2\varphi + \frac{2}{\rho^6}\right) - \sin\varphi\cos\varphi \left(\frac{1}{\rho\sin\theta}\frac{\partial\rho}{\partial\varphi}\right)\right] \\ A_3 &= \sin^2\theta \left(\sin^2\varphi - \frac{1}{\rho^6}\right) - 2\sin\theta\sin\varphi\cos\varphi \left(\frac{1}{\rho\sin\theta}\frac{\partial\rho}{\partial\varphi}\right) \\ &\quad + \left(\cos^2\varphi - \frac{1+3\cos^2\theta}{\rho^6}\right)\left(\frac{1}{\rho\sin\theta}\frac{\partial\rho}{\partial\varphi}\right)^2 \end{aligned}\right\} \tag{7}$$

and

$$\left.\begin{aligned} B_1 &= \cos^2\varphi - \frac{1+3\cos^2\theta}{\rho^6} \\ B_2 &= -2\sin\varphi\cos\varphi \left(\sin\theta - \frac{\cos\theta}{\rho}\frac{\partial\rho}{\partial\theta}\right) \\ B_3 &= \sin^2\varphi \left(\sin\theta - \frac{\cos\theta}{\rho}\frac{\partial\rho}{\partial\theta}\right)^2 - \frac{1}{\rho^6}\left(\sin\theta + \frac{2\cos\theta}{\rho}\frac{\partial\rho}{\partial\theta}\right)^2 \end{aligned}\right\} \tag{8}$$

The quadratic equations, equations (5) and (6), may be solved algebraically for the indicated variables, thus leading to the differential equations

$$\frac{1}{\rho}\frac{\partial\rho}{\partial\theta} = \frac{-A_2 \pm \sqrt{A_2^2 - 4A_1A_3}}{2A_1} \tag{9}$$

$$\frac{1}{\rho\sin\theta}\frac{\partial\rho}{\partial\varphi} = \frac{-B_2 \pm \sqrt{B_2^2 - 4B_1B_3}}{2B_1} \tag{10}$$

It should be noted that equations (9) and (10) are each, in actuality, two differential equations, due to the appearance of both the plus and minus signs

preceding the radical terms. The trace in the plane $\varphi = \pm\pi/2$, discussed previously (see fig. 2(a)), is given by solutions of the two ordinary differential equations to which equation (9) reduces in this case. The circular portion is a solution to the equation with the upper sign, and the remaining portion of this trace is a solution to the equation with the lower sign. As noted previously, the two portions intersect at a point forward of the polar axis that corresponds to a neutral point. The magnetic field in this trace of the boundary is proportional to $[\sin\theta + 2(\cos\theta/\rho)(\partial\rho/\partial\theta)]/\rho^3$, and it is evident that the alternative signs are related to the reversal of the direction of the field vector at the point of intersection of the two segments of this trace.

It is to be expected, then, that the complete approximate boundary will be composed of two surfaces that intersect, or in some manner merge, in the vicinity of the point over the pole, and that one of these surfaces will be a solution of equation (9) (or (10)) with the upper sign, and that the other surface will be a solution with the lower sign. The curve on the boundary along which the signs must be switched cannot be determined simply, so both surfaces must be computed independently. The boundary is then considered to be the exterior part of the two intersecting surfaces.

NUMERICAL INTEGRATION OF THE DIFFERENTIAL EQUATIONS

The solutions to equations (9) and (10) that represent the magnetosphere boundary are determined by an integration technique based on Euler's method for solving ordinary differential equations. (See, e.g., Kunz, ref. 17.) The application of this technique to the present problem will be described specifically for equation (9). It is to be understood, however, that the description applies as well for the solution of equation (10) except that the roles of the variables θ and φ are interchanged.

Equation (9) is of the general form

$$\partial\rho/\partial\theta = F[\rho, \theta, \varphi, (\partial\rho/\partial\varphi)] \tag{11}$$

The integration of this equation commences at a known trace of the desired solution in some surface θ = constant, for example, the plane $\theta = \pi/2$ in the present problem. Values for ρ are given at increments $\Delta\varphi$ along this trace, and the derivative $\partial\rho/\partial\varphi$ is computed by numerical differentiation. The derivative $\partial\rho/\partial\theta$ is now readily determined by means of equation (11). A step $\Delta\theta$, from the surface $\theta = \theta_i$ to the surface $\theta = \theta_{i+1}$, is taken by inserting the values for ρ_i, θ_i, φ_i, and $(\partial\rho/\partial\theta)_i$ into the linear extrapolation formula

$$\rho_{i+1} = \rho_i + \Delta\theta(\partial\rho/\partial\theta)_i \tag{12}$$

The derivatives $(\partial\rho/\partial\varphi)_{i+1}$ and $(\partial\rho/\partial\theta)_{i+1}$ are now calculated by the methods stated above, and refined values for ρ_{i+1} are obtained by substitution into the averaging extrapolation formula

$$\rho_{i+1} = \rho_i + (\Delta\theta/2)[(\partial\rho/\partial\theta)_i + (\partial\rho/\partial\theta)_{i+1}] \qquad (13)$$

New values for the derivatives of ρ_{i+1} are computed as before, and the extrapolation-integration process is repeated for succeeding steps $\Delta\theta$.

Attention should be called to the fact that the coefficients A_1 and A_2 in equation (9) vanish for $\theta = 90^\circ$. Thus, equation (9) is indeterminate at the trace in the plane $\theta = 90^\circ$, and tends to be sensitive to small errors near this trace. The derivative $\partial\rho/\partial\varphi$, equation (10), is zero in the plane $\varphi = \pm 90^\circ$, by consideration of symmetry. The numerator of equation (10) should therefore vanish at $\varphi = \pm 90^\circ$. Small errors in the vicinity of the trace in the plane $\varphi = \pm 90^\circ$ may lead to negative values for the discriminant $B_2^2 - 4B_1B_3$, however, thus limiting the use of equation (9) near these traces. Both equations are poorly conditioned near the polar axis, in that small errors may lead to negative numbers under square root signs. It is due to these complications that integrations could not be started in the polar region of the trace in the plane $\varphi = 90^\circ$, nor from the segment $\varphi > 180^\circ$ of the trace in the plane $\theta = 90^\circ$. Thus, the boundary could not be determined by single integrations commencing on one or the other of the planes of symmetry, but was calculated in several pieces, as described in the next section of this paper.

The numerical computations have been carried out with the use of an IBM 7090 computer in the region $90^\circ \leq \varphi \leq 270^\circ$, $0 \leq \theta \leq 90^\circ$. The machine procedure employed for the taking of derivatives numerically is SHARE Subroutine CL SMD 3, Distribution no. 331, which has been converted for FORTRAN use. This program involves a 7-point polynomial smoothing process, followed by a three-point differentiation process, and it has been found to give good results in quite general application.

RESULTS AND DISCUSSION

The sunward, nearly hemispherical, portion of the boundary was calculated with the use of equation (9), starting on the segment $90^\circ \leq \varphi \leq 180^\circ$ of the trace in the plane $\theta = 90^\circ$ (see fig. 2(b)). The integration was performed in the direction of decreasing θ. The upper sign was chosen to precede the radical term in the differential equation, by analogy with this choice in the computation of the circular part of the trace in the plane $\varphi = 90^\circ$. The increments $\Delta\theta$ and $\Delta\varphi$ were 2.5° and 5°, respectively. At $\theta = 20^\circ$ the integration was halted because of the occurrence of negative values of the discriminant $A_2^2 - 4A_1A_3$ for φ in the range $90^\circ \leq \varphi \leq 135^\circ$. Two additional integrations were carried out starting from the segments $135^\circ \leq \varphi \leq 180^\circ$ and $150^\circ \leq \varphi \leq 180^\circ$ of the trace in the plane $\theta = 90^\circ$. The increments $\Delta\theta$ and $\Delta\varphi$ were taken to be 2° and 2.5°, respectively, in these two computations. The first of these was stopped at $\theta = 18^\circ$, and the second at $\theta = 14^\circ$, because of the occurrence, again, of negative values for the above indicated expressions.

It was noted earlier that the trace in the plane $\varphi = 90^\circ$ consists of two intersecting curves obtained with the use of both of the differential equations

implicit in equation (10). The integrations discussed in the foregoing paragraph might possibly have been continued to the point over the pole if it were known at precisely what point in each plane φ = constant (e.g., the point N in the plane $\varphi = 90^\circ$, shown in figure 2(a)) to switch to the other of the two differential equations. The curve in the surface along which the switching takes place cannot be determined by any simple technique, however, so the polar portion of the boundary must be calculated by other means. There remains, also, the computation of the coordinates in the region $180^\circ \leq \varphi \leq 270^\circ$.

It was found that the trace previously obtained in the range $14^\circ \leq \theta \leq 90^\circ$ in the plane $\varphi = 180^\circ$ can be joined smoothly to the point $\rho = 2^{1/3}$ on the polar axis by means of a curve defined by the simple relation

$$\rho = 2^{1/3} + K\theta^2 \tag{14}$$

The constant K is evaluated by substitution into this relation of the value for ρ at some point, say $\theta = 20^\circ$, on the previously determined portion of the trace in this plane. Equation (10) was used to calculate the coordinates of the boundary in the region $180^\circ \leq \varphi < 270^\circ$ commencing with the trace in plane $\varphi = 180^\circ$ as discussed above. The negative sign is chosen to precede the radical term, by analogy with the simpler computation of the trace in the plane $\theta = 90^\circ$. (See, e.g., ref. 6, 10, or 11.)

The integration was performed in the range $0 \leq \theta \leq 90^\circ$ in the direction of increasing φ, with the increments $\Delta\theta = 2^\circ$ and $\Delta\varphi = 5^\circ$. The process yielded results up to the plane $\varphi = 255^\circ$. A second computation was performed with $\Delta\theta$ taken to be 5°. These results agree to at least three significant figures with the first integration. A third integration was carried out in the range $0 \leq \theta \leq 20^\circ$, where $\Delta\theta$ and $\Delta\varphi$ were taken to be 2° and 5°, respectively. The integration produced results up to the plane $\varphi = 265^\circ$ which agree to at least three significant figures with the overlapping computations previously discussed.

The coordinates of the boundary in the region $90^\circ \leq \varphi < 180^\circ$, near the polar axis, were computed by integrations from an assumed trace in the plane $\varphi = 135^\circ$. The starting trace was chosen by trial and error such that the calculated traces near the plane $\varphi = 90^\circ$ approached the known trace in the plane $\varphi = 90^\circ$ as closely and smoothly as possible. Equation (10) was used here, with the upper sign. The starting trace was given in the range $0 \leq \theta \leq 20^\circ$, and the increments $\Delta\theta$ and $\Delta\varphi$ were 2° and 1°, respectively. The computations were stopped at the plane $\varphi = 99^\circ$ in the approach to the plane $\varphi = 90^\circ$, and at the plane $\varphi = 168^\circ$ in the approach to the plane $\varphi = 180^\circ$. The resulting surface merges smoothly into the lower nearly hemispherical portion, as previously calculated, for φ greater than about 150°. The values for ρ at the plane $\varphi = 99^\circ$ were extrapolated linearly, by means of equation (12), over an increment $\Delta\varphi = -9^\circ$ to the plane $\varphi = 90^\circ$. These results agree to three significant figures with the known analytic solution in this plane.

The results of these integrations are shown in figure 3 in the form of traces in the planes $\varphi = 90^\circ, 105^\circ, 120^\circ, \ldots, 270^\circ$. The traces in the planes $\varphi = 90^\circ$ and 270° are the analytic solutions shown in figure 2(a), and the point labeled N corresponds to the neutral point in the exact solution to the

Chapman-Ferraro problem. Notice that in the region $90^\circ \leq \varphi < 150^\circ$ the polar portion of the boundary intersects the main sunward portion with discontinuous slope $\partial\rho/\partial\theta$. This discontinuity unquestionably represents a failure of the present approximation, and would not exist in the exact solution. It is believed, however, that this is a local failure, and that the present approximate results should be in substantial agreement with solutions to the exact problem over nearly all of the boundary. Numerical values for ρ as a function of θ in planes of constant φ are presented in table I.

FIELD LINES IN THE MAGNETOSPHERE

A computation of field lines in the magnetic meridian plane containing the free-stream direction will be described in the following paragraphs.

According to the Chapman-Ferraro geomagnetic storm theory, the field $\underset{\sim}{B}$ must exhibit a dipole singularity at the origin and satisfy the relations curl $\underset{\sim}{B} = 0$ and div $\underset{\sim}{B} = 0$. At the boundary, which forms as a result of interaction with the solar wind, the normal component of $\underset{\sim}{B}$ must vanish and the tangential component must satisfy equation (1). If the boundary has been determined so as to satisfy these boundary conditions, then the field $\underset{\sim}{B}$ inside the boundary can be determined by solution of the above boundary-value problem. Alternatively, but equivalently, it may be determined by summing the effects of the geomagnetic dipole and the currents flowing in the boundary by means of the equation

$$\underset{\sim}{B} = \underset{\sim}{B}_p + \int_S \frac{\underset{\sim}{J}\times\bar{d}}{|\bar{d}|^3}\, dS \tag{15}$$

where $\underset{\sim}{B}_p$ represents the geomagnetic dipole and $\bar{d}$ is the vector from the point at which the field is to be determined to points on the boundary. The symbol $\underset{\sim}{J}_s$ represents the currents in the boundary, and it is related to the tangential field $\underset{\sim}{B}_s$ by the equation

$$\underset{\sim}{J}_s = \underset{\sim}{B}_s\times\hat{n}/4\pi \tag{16}$$

where $\hat{n}$ is an outwardly directed unit vector normal to the boundary. The integration in equation (15) is to be carried out over the entire boundary. The results for $\underset{\sim}{B}$ by the two methods described above will be identical, and field lines may be computed by solution of the differential equations

$$\frac{dy}{ds} = \frac{B_y}{|\underset{\sim}{B}|}, \qquad \frac{dz}{ds} = \frac{B_z}{|\underset{\sim}{B}|} \tag{17}$$

where B_y and B_z are the y and z components of $\underset{\sim}{B}$, and s is a running variable along the field line.

The exact condition that the normal component of $\underset{\sim}{B}$ at the boundary is zero has been replaced, in the present boundary computation, by the approximate condition given by equation (2). If, now, $\underset{\sim}{J}_s$ is evaluated by means of equation (16),

where $\underset{\sim}{B}_s$ is consistent with equation (2) and the approximately determined boundary, then field lines may be determined by use of equations (15) and (17). Alternatively, the calculated boundary may be considered to be exact, and the field may then be calculated by solution of the previously stated boundary-value problem. Since the shape of the boundary has been determined only approximately, the two sets of resulting values for the enclosed magnetic field will be different. The first mentioned method, involving the use of equations (15) and (16), is the simpler of the two to apply, and will be employed here.

The constant f is arbitrary in the approximate boundary calculation, and its value may be chosen so as to improve the compatibility of the boundary and the field lines in local regions. In the present case, f was selected to assure that none of the field lines cross the boundary on the sunward side. The value so chosen is 0.85.

The results for several field lines are presented in figure 4. A few field lines corresponding to the undistorted dipole are also shown for comparison. These computations are plotted in terms of the dimensionless variable ρ. Figure 4 is a universal plot, for the given value of f, for all values of n and v. The radius of the earth, ρ_e, depends upon the quantity r_o (eq. (4)), however. The field lines are labeled, for convenience, with the polar angle θ_e at which they intersect the earth, under the assumption that r_o is 9.0 earth radii. This case, which forms the basis for the drawing of the earth in figure 4, occurs, for instance, for values of n and v of 2.5 protons/cm^3 and 500 km/sec, assuming that f = 0.85.

A gross characteristic of the computed field is that geomagnetic dipole lines of force are compressed on both the daytime and nighttime sides because of the magnetic effect of electric currents in the boundary. Another is that field lines that intersect the earth within about 7° of the polar axis on the sunward side are swept rearward. As stated previously, the constant f was chosen so that none of the lines of force cross the boundary on the sunward side. The compatibility between the approximate boundary and the field lines is thus seen to be good forward of the neutral point N. The pattern of field lines tends to recede from the boundary from the neutral point rearward, however. It would appear, therefore, that the height z of the boundary indicated by the present approximate results is somewhat greater than would be given by an exact solution of the Chapman-Ferraro problem. This conclusion is supported, furthermore, by the fact that the exact solution would indicate that the boundary is parallel to the direction of the undisturbed solar wind at the neutral points and that the maximum height of the boundary infinitely far downstream must be twice the height at the neutral point. Thus, a lowering of the point N, consistent with the implications of the calculated field lines, would be reflected in a general decrease of the height of the entire rear portion of the boundary. It is anticipated, however, that except in the immediate vicinity of the boundary, and far downstream from the earth, the present field computations should provide a useful approximation to the results that may be anticipated when the Chapman-Ferraro problem is ultimately solved exactly.

Ames Research Center
National Aeronautics and Space Administration
Moffett Field, Calif., April 26, 1963

REFERENCES

1. Chapman, Sydney: Idealized Problems of Plasma Dynamics Relating to Geomagnetic Storms. Reviews of Modern Physics, vol. 32, no. 4, Oct. 1960, pp. 919-933.

2. Ferraro, V. C. A.: Theory of Sudden Commencements and of the First Phase of a Magnetic Storm. Reviews of Modern Physics, vol. 32, no. 4, Oct. 1960, pp. 934-940.

3. Dungey, J. W.: Cosmic Electrodynamics. Cambridge University Press, 1958.

4. Chapman, S., and Kendall, P. C.: An Idealized Problem of Plasma Dynamics that Bears on Geomagnetic Storm Theory; Oblique Projection. Jour. Atmospheric and Terrestrial Physics, vol. 22, no. 2, Oct. 1961, pp. 142-156.

5. Parker, E. N.: Dynamics of the Geomagnetic Storm. Space Science Reviews, vol. 1, no. 1, June 1962, pp. 62-99.

6. Beard, David B.: The Interaction of the Terrestrial Magnetic Field With the Solar Corpuscular Radiation. Jour. Geophys. Res., vol. 65, no. 11, Nov. 1960, pp. 3559-3568.

7. Beard, David B.: The Interaction of the Terrestrial Magnetic Field With the Solar Corpuscular Radiation, 2 Second-Order Approximation. Jour. Geophys. Res., vol. 67 , no. 2, Feb. 1962, pp. 477-483.

8. Beard, David B., and Jenkins, Edward B.: Correction to the Second Approximation Calculation of the Geomagnetic Field, Solar Wind Interface. Jour. Geophys. Res., vol. 67, no. 12, Nov. 1962, pp. 4895-4896.

9. Ferraro, V. C. A.: An Approximate Method of Estimating the Size and Shape of the Stationary Hollow Carved out in a Neutral Ionized Stream of Corpuscles Impinging on the Geomagnetic Field. Jour. Geophys. Res., vol. 65, no. 12, Dec. 1960, pp. 3951-3953.

10. Spreiter, John R., and Briggs, Benjamin R.: Theoretical Determination of the Form of the Hollow Produced in the Solar Corpuscular Stream by Interaction With the Magnetic Dipole Field of the Earth. NASA TR R-120, 1961.

11. Spreiter, John R., and Briggs, Benjamin R.: Theoretical Determination of the Form of the Boundary of the Solar Corpuscular Stream Produced by Interaction With the Magnetic Dipole Field of the Earth. Jour. Geophys. Res., vol. 67, no. 1, Jan. 1962, pp. 37-51.

12. Spreiter, John R., and Briggs, Benjamin R.: On the Choice of Condition to Apply at the Boundary of the Geomagnetic Field in the Steady-State Chapman-Ferraro Problem. Jour. Geophys. Res., vol. 67, no. 7, July 1962, pp. 2983-2985.

13. Davis, Leverett, Jr., and Beard, David B.: A Correction to the Approximate Condition for Locating the Boundary between a Magnetic Field and a Plasma. Jour. Geophys. Res., vol. 67, no. 11, Oct. 1962, pp. 4505-4507.

14. Neugebauer, Marcia, and Snyder, Conway W.: The Mission of Mariner II: Preliminary Observations, Solar Plasma Experiment. Science, vol. 138, no. 3545, Dec. 1962, pp. 1095-1097.

15. Axford, W. I.: The Interaction between the Solar Wind and the Earth's Magnetosphere. Jour. Geophys. Res., vol. 67, no. 10, Sept. 1962, pp. 3791-3796.

16. Kellogg, P. J.: Flow of Plasma Around the Earth. Jour. Geophys. Res., vol. 67, no. 10, Sept. 1962, pp. 3805-3811.

17. Kunz, Kaiser S.: Numerical Analysis. McGraw-Hill Book Co., Inc., New York, 1957.

TABLE I.- VALUES OF ρ IN PLANES φ = CONSTANT

θ, deg	φ, deg												
	90	105	120	135	150	165	180	195	210	225	240	255	270
0	1.260	1.260	1.260	1.260	1.260	1.260	1.260	1.260	1.260	1.260	1.260	1.260	1.260
5	1.186	1.186	1.193	1.205	1.220	1.235	1.260	1.280	1.299	1.316	1.330	1.339	1.341
10	1.116	1.121	1.137	1.159	1.190	1.227	1.261	1.300	1.340	1.375	1.404	1.425	1.430
15	1.051	1.057	1.079	1.112	1.155	1.211	1.264	1.322	1.382	1.438	1.484	1.520	1.528
20	1.000	1.013	1.044	1.085	1.136	1.197	1.269	1.340	1.425	1.504	1.572	1.624	1.639
25	1.000	1.009	1.034	1.073	1.126	1.194	1.277	1.367	1.469	1.573	1.667	1.739	1.764
30	1.000	1.008	1.031	1.068	1.122	1.193	1.285	1.390	1.513	1.646	1.772	1.869	1.907
35	1.000	1.007	1.030	1.066	1.120	1.195	1.294	1.413	1.558	1.722	1.887	2.083	2.075
40	1.000	1.007	1.030	1.066	1.120	1.197	1.303	1.434	1.601	1.801	2.015	2.198	2.273
45	1.000	1.007	1.030	1.066	1.121	1.200	1.312	1.454	1.643	1.882	2.156	2.408	2.514
50	1.000	1.007	1.030	1.066	1.122	1.203	1.320	1.473	1.683	1.964	2.312	2.652	2.814
55	1.000	1.007	1.030	1.067	1.124	1.206	1.327	1.490	1.720	2.045	2.484	2.953	3.197
60	1.000	1.007	1.030	1.067	1.125	1.208	1.333	1.505	1.754	2.124	2.671	3.329	3.707
65	1.000	1.007	1.031	1.068	1.126	1.211	1.339	1.517	1.784	2.197	2.865	3.788	
70	1.000	1.007	1.031	1.068	1.127	1.213	1.343	1.528	1.810	2.256	3.044		
75	1.000	1.007	1.031	1.068	1.128	1.214	1.347	1.536	1.830	2.313	3.222		
80	1.000	1.007	1.030	1.069	1.129	1.215	1.349	1.542	1.845	2.357	3.370		
85	1.000	1.007	1.030	1.069	1.129	1.218	1.349	1.544	1.853	2.388	3.473		
90	1.000	1.007	1.030	1.069	1.130	1.219	1.349	1.545	1.855	2.392	3.500		

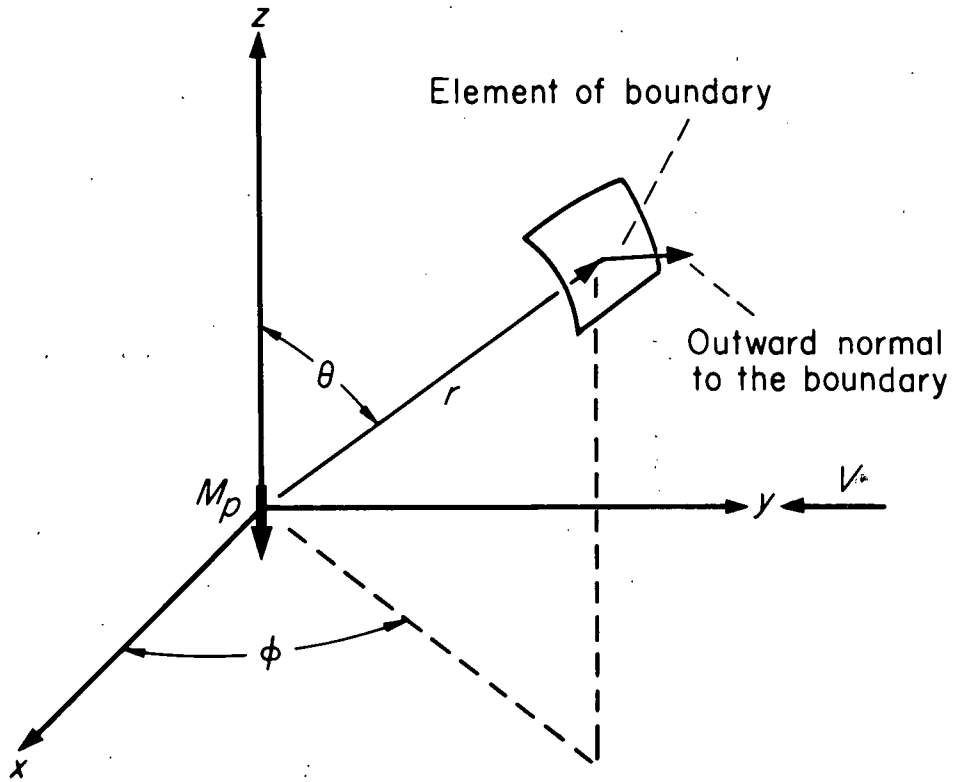

Figure 1.- The coordinate system.

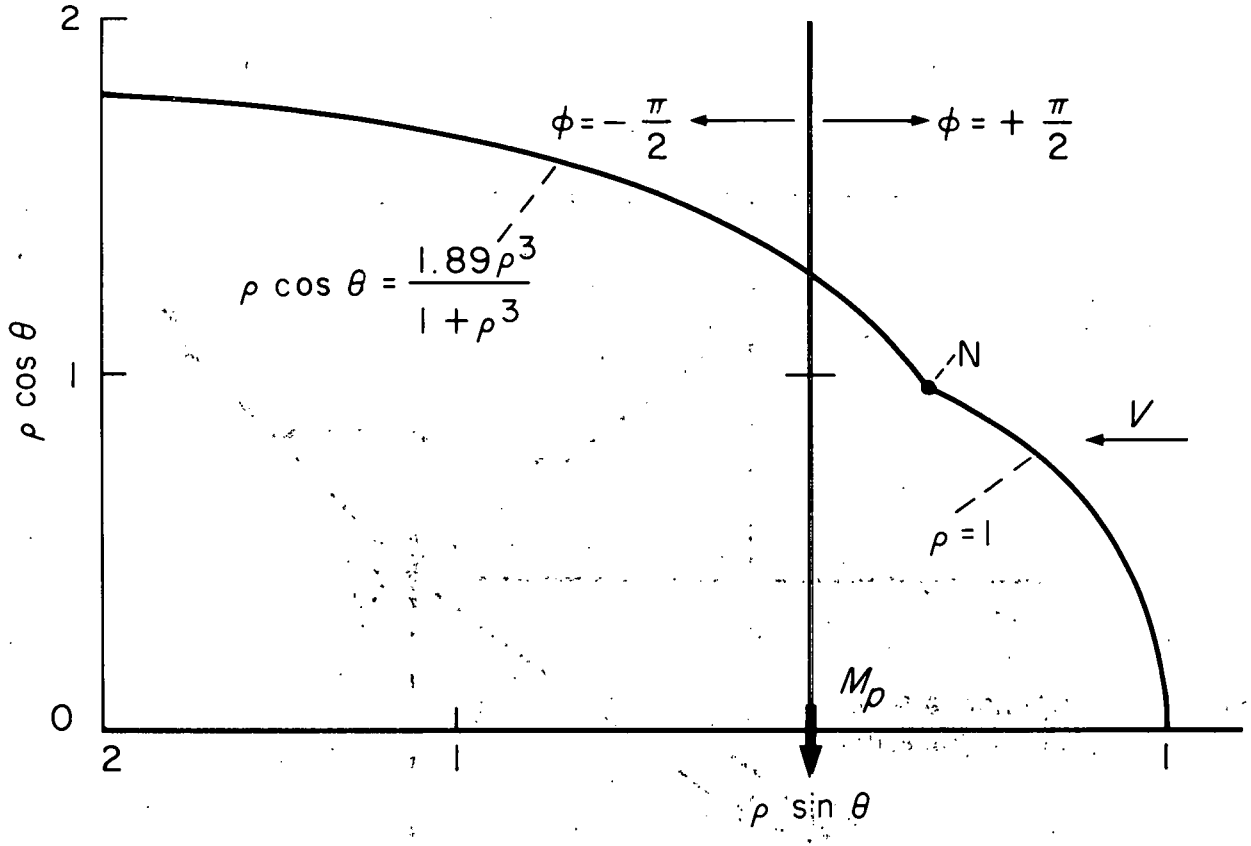

(a) Magnetic meridian plane containing the free-stream direction, $\varphi = \pm\pi/2$.

Figure 2.- Analytic solutions in the planes of symmetry of the boundary.

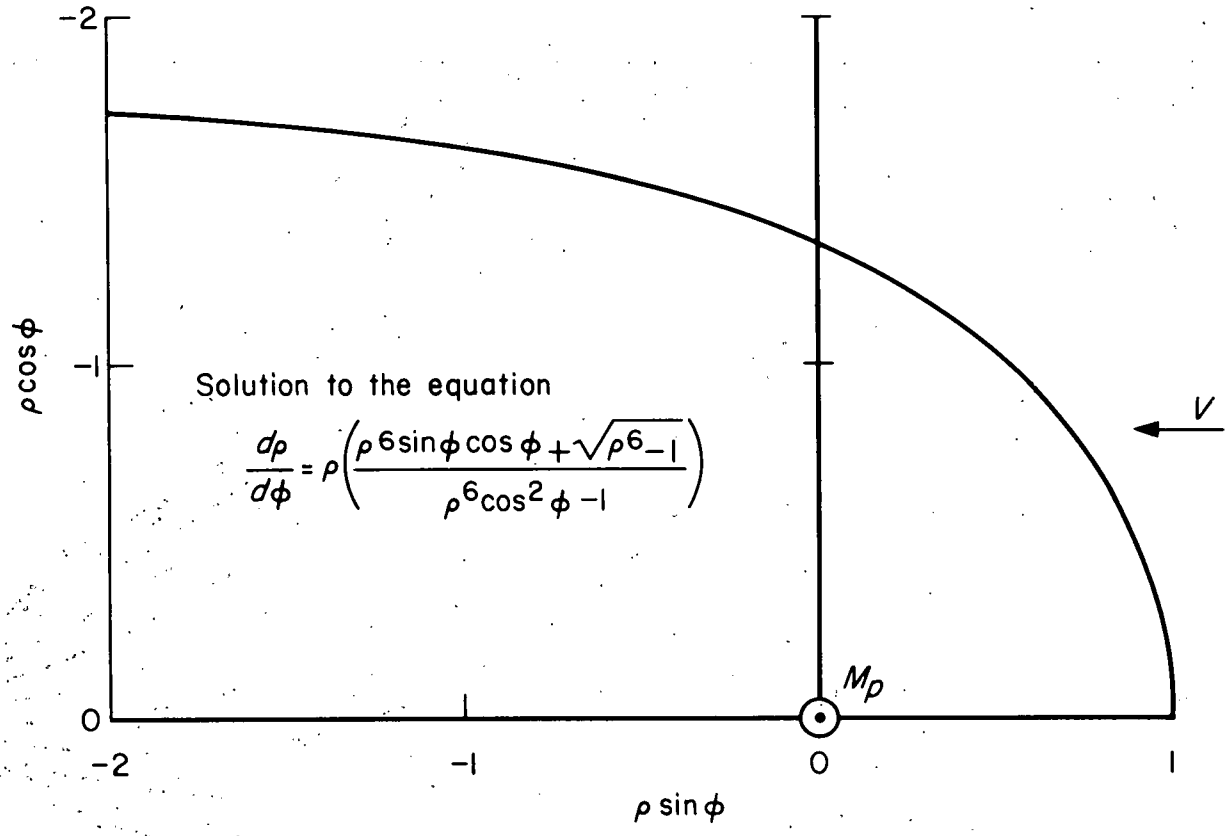

(b) Equatorial plane, $\theta = \pi/2$.

Figure 2.- Concluded.

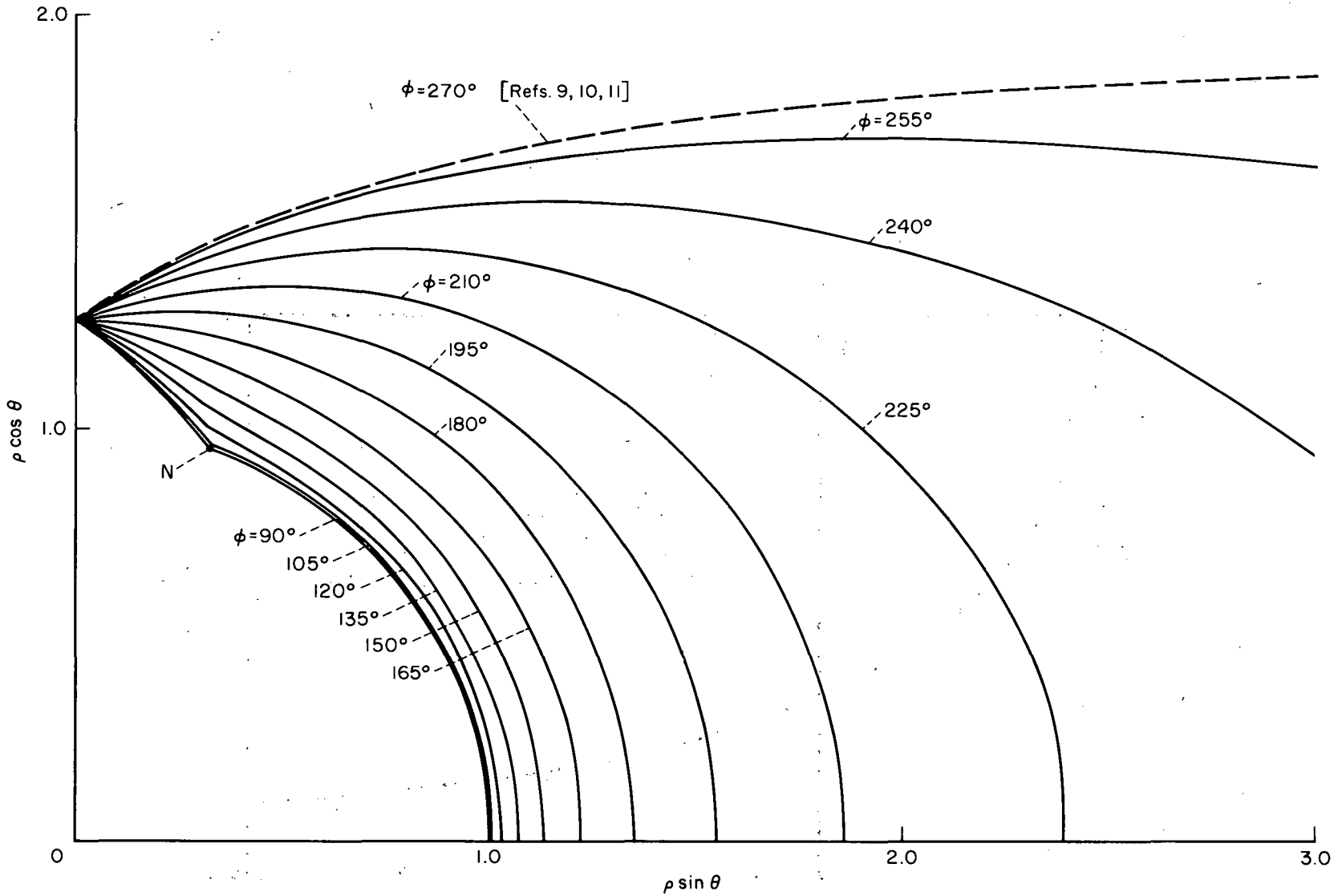

Figure 3.- Traces of the boundary of the magnetosphere in planes of constant angle φ.

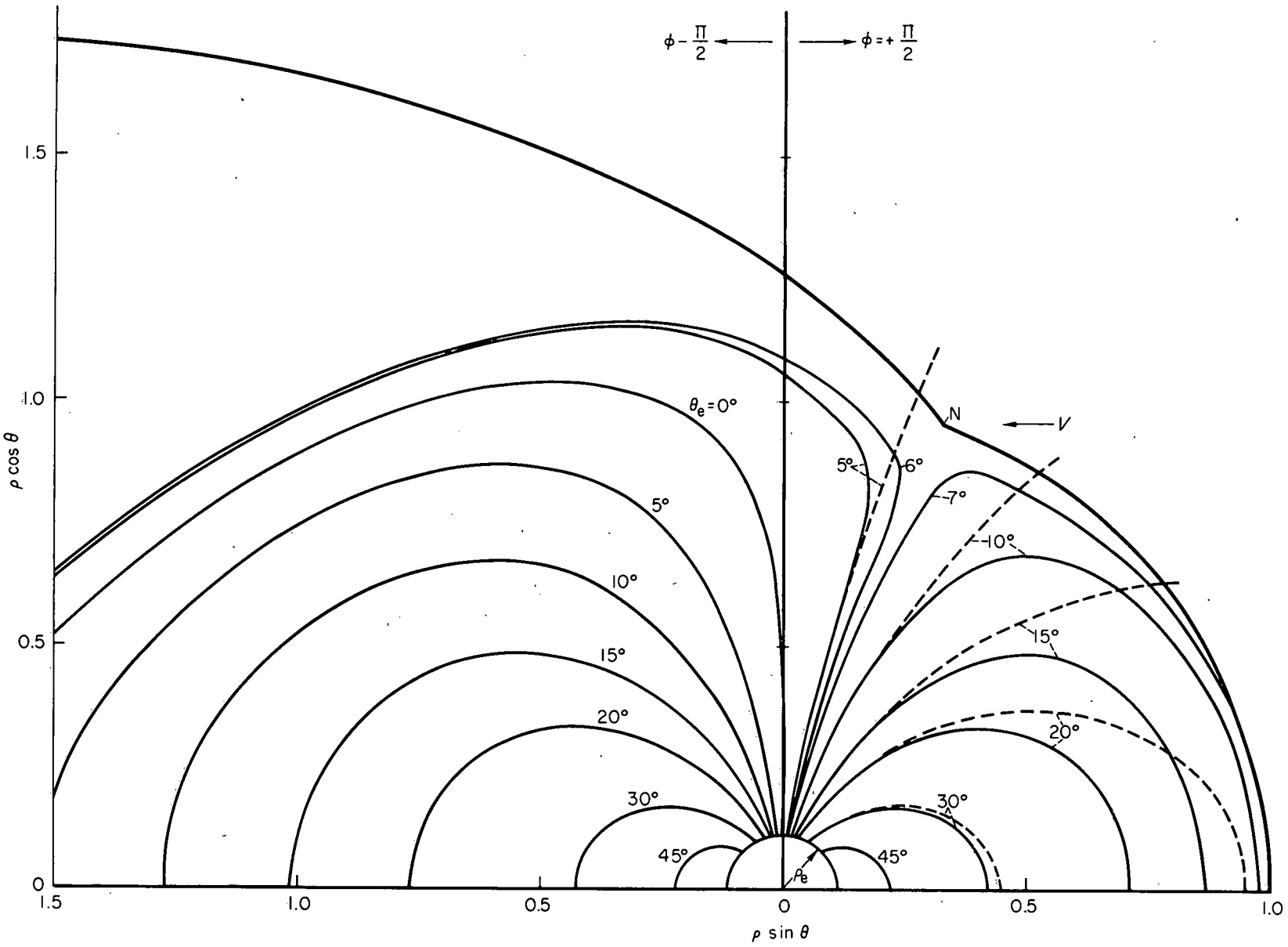

Figure 4.- Field lines in the magnetic meridian plane containing the free-stream direction.